energyequipsys/ Vol 4/No1/June 2016/ 11-19

ENERGY EQUIPSYS

Energy Equipment and Systems

http://energyequipsys.ut.ac.ir
www.energyeuquipsys.com

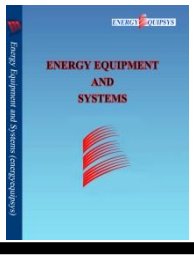

Evaluation of solid oxide fuel cell anode based on active triple phase boundary length and tortuosity

Authors

Ali Hasanabadi [a]
Majid Baniassadi [a*]
Karen Abrinia [a]
Mostafa Baghani [a]
Mohsen Mazrouei Sebdani [a]

[a] School of Mechanical Engineering, College of Engineering, University of Tehran, P.O. Box 111554563, Tehran, Iran

Article history:

Received : 2 February 2016
Accepted : 21 February 2016

ABSTRACT

An efficient procedure is presented for the evaluation of solid oxide fuel cell (SOFC) anode microstructure triple phase boundary length (TPBL). Triple phase boundary- the one that is common between three phases of the microstructure- has a great influence on the overall efficiency of SOFC because all electrochemical reactions of anode take place in its vicinity. Therefore, evaluation of TPBL for virtual or experimental 3D microstructures is essential for comparison purposes and the optimization processes. In this study, first, an algorithm is proposed to distinguish between percolated and non-percolated clusters for each of the phases. Then, another algorithm is used to determine the value of TPBL for all percolated clusters of three phases. Also, a procedure based on thermal and diffusion analogy is presented to assess the tortuosity of porous and solid phases. Finally for a virtual microstructure, percolated clusters, active and total TPBL and tortuosity are calculated and discussed.

Keywords: Active Triple Phase Boundary Length, Anode, Active Cluster, Solid Oxide Fuel Cell, Tortuosity.

1. Introduction

Solid oxide fuel cell (SOFC) is an electrochemical device that is used for the conversion of chemical energy of fuel into electricity with high efficiency compared to traditional technologies. The high energy conversion efficiency of SOFC, together with their high fuel flexibility (hydrogen, hydrocarbons, carbon monoxide, etc.), make them an ideal candidate for a better exploitation of fossil fuels, and for an efficient conversion of renewable energy sources into electricity [1, 2]. Production of electricity using a low-cost, clean and high efficiency process has created motivation for researchers on all relevant aspects of SOFC [3-13].

*Corresponding author: Majid Baniassadi
Address: School of Mechanical Engineering, College of Engineering, University of Tehran, P.O. Box 111554563, Tehran, Iran
E-mail address: m.baniassadi@ut.ac.ir

SOFC is essentially consisted of three main parts: two porous electrodes, separated by a dense oxide ion conducting electrolyte. The main reaction of SOFC is oxidation of the fuel. On the cathode side, oxygen gas molecules react with incoming electrons coming from external circuit. Output of this reaction is oxygen ions which migrate through the electrolyte to the anode. It is clear that the electrolyte must be ion conducting. At the anode, the oxide ions react with an appropriate fuel such as H_2. Outputs of this reaction are H_2O and electrons. The electrons flow from anode to the cathode through the external circuit to produce electricity. If both oxygen and fuel are provided continuously, the SOFC can steadily generate electricity [14].

Based on the function of SOFC, the role of anode is providing an excellent catalyst for oxidation of the fuel. In addition, it must have

the capability of conducting electrons and ions and sufficient porosity to allow gas species pass through it. Other requirements include stability in the chemical environment, matching the thermal expansion coefficients of anode and electrolyte, chemical stability, and applicability of various fuels [14].

In a three-phase SOFC anode consisting of Nickle (Ni) and yttria-stabilized zirconia (YSZ), Ni is the electron conducting element. YSZ is ion-conducting element and void has the responsibility of transporting fuel. It is a common belief that the oxidation reaction of fuel occurs only near the triple phase boundary (TPB) where the three phases are present. Presenting an efficient and accurate method for calculating triple-phase boundary length (TPBL) is the subject of this article.

Mazrouei et al. [15] using an artificial neural network and genetic algorithm, found a microstructure with maximum active TPBL. They generated a series of virtual realizations for anode microstructure using Monte Carlo methodology and by evaluating these microstructures based on TPBL, they found the optimal microstructure.

Deng et al. [16] developed a geometrical model to predict the influences of solid grain size, pore size and porosity on the TPBL in electronic composite electrodes of SOFC. They concluded that a finer solid grain size increases the TPBL and the optimal value of this factor depends on grain sizes, pore sizes, and porosity value. Despite the attained correct conclusions, the proposed method suffers some basic flaws. They assumed the entire pore space as spherical grains and they equated the surface of all these grains to the surface of the solid phase which is not correct. Also in their assumed model the overlap value of two spheres, that is an important parameter, was set to a value without any rational analysis.

Janardhanan et al. [17] presented a mathematical model to calculate the volume specific TPBL in the porous composite electrodes of SOFC. The model is exclusively based on geometrical considerations accounting for porosity, particle diameter, particle size distribution, and solids phase distribution. They considered uniform particle size distribution as well as the non-uniform one for the calculation of volume specific TPBL. Even though the proposed modeling is better than the Deng method [16] the fractional overlap is not determined either.

Digitized microstructures are presented by a number of voxels. Every edge of a voxel is surrounded with three other voxels. With the assumption that every voxel is occupied by only one phase, the aforementioned edge is considered a TPB segment if the neighboring four voxels comprise all three phases. Because of the step like pattern of the voxelized microstructures, if the TPB segments are simply added up, the total length of TPB is overestimated. Some researchers have proposed a correction factor to attain the real TPBL.

Golbert et al. [18] counted all the pixels neighboring a TPB edge (four per edge) and divided this overall number by four. This approach reduces the calculated TPB length since some pixels appear for more than one edge but are only counted once.

Suzue et al. [19] assumed that, geometrically, the actual TPB length should lie between 57.7% and 100% of the cubic voxel perimeter. Therefore, they reduced the calculated TPBL by 20% as a representative value.

Wilson et al. [20], using an analytical assumption for calculated and actual TPBL, concluded that the average value for correction factor is about 1.455. They assumed that the TPBL, calculated in a voxelized media for any direction, is the sum of the coordinate components of its respective vector. Therefore, they attained the average correction factor by integrating in all directions on the unite sphere.

To correct the overestimated TPBL, some researchers used summation of other distances such as midpoint lengths or centroid point lengths [21, 22]. Shikazono [21] proposed that instead of simply summing up TPB segments, the actual TPBL is calculated using the total connection lengths of the midpoint of TPB edge segment or the total distance between the centroids of the triangles defined by the neighboring midpoints of the edge segments. Using TPB of two overlapped spheres, they compared three methods and concluded that the centroid method could calculate the TPBL within 5% error.

In this study, first, an efficient algorithm was presented for identifying active clusters for each phase. Then, based on active clusters, another algorithm was presented for active TPBL calculations. Because of considering only active clusters, the attained TPBL will be the active one. This was followed by using a thermal conductivity analogy, calculating and discussing the efficient diffusion coefficient. Finally, for a virtual microstructure, active TPBL and tortuosity were calculated.

2. Identifying Active Clusters

A cluster of a phase is a subset of that phase in such a way that every pair could be connected to each other without crossing other phases. A cluster is active and percolated in a direction (for example z) where there is at least one point, belonging to that cluster, on each plane of $z = 0$ and $z = z_{max}$. The behavior of effective properties such as transport (conductivity, diffusion, and fluid permeability) and elastic (Young's modulus) ones are affected by the percolation of respective phases.

To determine the cluster of a specified phase (for example, black in Fig. 1), the algorithm is started from the first cell on the top left (for the first column and row, an additional column and row is added (the orange color column and row in Fig. 1) so that the algorithm could work correctly). If this cell is occupied by the other phases, the next bottom cell is considered and this continues to reach the cell that belongs to the specified phase. Upon reaching the desired cell, first, the phase of this cell is compared with the left and top cells only and, based on the conditions, there will be three situations. If the phase of the considered cell is different from both left and top cells, it is assigned a new cluster number. If it is similar to one of the two cells, the cluster number of these similar cells will be considered identical. If the phase of all cells (top, left, and the considered one) are identical and the cluster number of top and left cells are dissimilar, one of the clusters (for example, left) will be omitted and all the cells related to this omitted cluster, together with the considered cell, will be assigned the cluster number of the fixed cell (top cell) (Fig. 1).

After determining the cluster of a cell, the next bottom cell is considered and the algorithm is continued. It should be noted that the movement direction of algorithm is always to the bottom and after finishing a column the next right bottom is considered.

This algorithm is almost similar to the cluster multiple labeling technique presented by Hoshen and Kopelman [23].

Cluster determination for three-dimensional media is basically similar to the two-dimensional media. For three-dimensions, determination of cluster number is carried out for each plane and after finishing a plane, the next top plane is considered for assessment. The movement directions of the algorithm are only on the positive side of coordinate axes.

3. Determining the Active TPBL

TPB is the common boundary of all phases. In order to determine active TPBL, first, active cluster of all phases must be determined. Considering only active clusters, the common boundary among them will be active too.

For easy counting of the TPB segment, the procedure is carried out in three steps. In each step only the unidirectional edges of voxelized microstructure are counted. For each assessed edge, if the presence of all phases in the four surrounding voxels is verified, that edge can be considered as a TPB segment (Fig. 2).

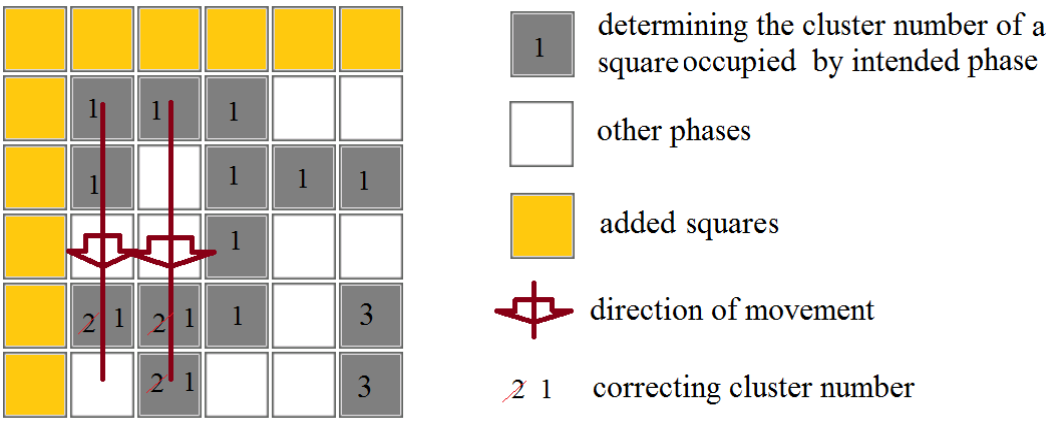

Fig. 1. Schematic of the implemented algorithm for identifying cluster number of an square occupied by an intended phase

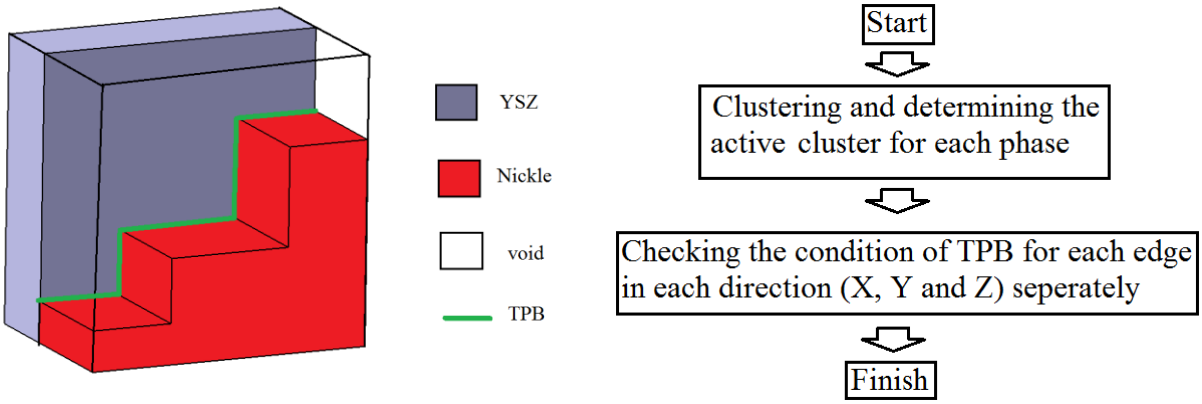

Fig. 2. (left) An edge is considered as TPB segment if all three phases are present in surrounding cells (right) schematic of the used algorithm for determining active TPB segments.

4. Effective Diffusion Coefficient and Tortuosity

Transportation of gas fuel, electron and ion are the essential geometrical issues for proper functioning of the SOFC anode. Phase percolation is a main factor that influences the effective coefficient of respective transportation.

The anode porous media provides pathways for flowing fuel gas through the structure. Because of the pore size of the porous media (about nanometer-to-micrometer), the main mechanism of gas transport is diffusion [5]. Depending on the characteristics of the diffusing gas species and microstructure morphology and scale, three mechanisms can occur when gas molecules travel through the porous media. These mechanisms are molecular diffusion, viscous diffusion, and Knudsen diffusion [5]. Among these mechanisms, a reasonable approximation for effective diffusion coefficient for the porous media can be calculated using [5]

$$\mathcal{D}^{eff} = \frac{\nu}{\tau}\,\mathcal{D}\,, \qquad (1)$$

where $\mathcal{D}^{eff}$, τ, and $\mathcal{D}$ are effective diffusion, tortuosity, and bulk diffusion coefficient, respectively.

Similar relations could be expressed for effective conduction coefficient of Nickle and YSZ phase. In the anode, every phase transports species apart from others. This means transportation of ion, electron, and gas fuel is carried out only through the YSZ-, Nickle- and void-phase, respectively, and other phases are insulator to what passes through the considered phase. Therefore, the tortuosity of each phase can be calculated separately from the others, using the thermal conductivity analogy. Effective diffusion problem of a distinct phase is mathematically equivalent to effective electrical and thermal conductivity problems in the cases where adjacent phases are nonconductor to what passes through the considered phase [24, 25].

A dimensionless factor, F, can be defined using the mathematical equivalency of thermal and diffusion problems as

$$F = \frac{\sigma}{\sigma^{eff}} = \frac{\mathcal{D}}{\mathcal{D}^{eff}}\,, \qquad (2)$$

where σ^{eff} and σ are the effective and bulk thermal conductivity coefficients of the specified phase, respectively.

For each phase, using thermal conductivity problem and assuming $\sigma = 1$, σ^{eff} and F could be computed for each direction.

In order to determine σ^{eff} for any intended direction, two different temperatures, as boundary conditions, are considered for the two surfaces perpendicular to the specified direction and all the other surfaces are assumed to be insulator.

Using Eqs. (1) and (2), the tortuosity can be expressed as:

$$\tau = F\,\nu. \qquad (3)$$

5. Results and Discussion

5.1. Evaluating the Percolated and Active Clusters of the Microstructure

For the implementation of the procedure, a virtual three-phase anode microstructure consisted of 26% Nickle, 33% YSZ, and 41% void with cell dimensions of 150x150x150 was used. Virtual realization of the microstructure was carried out by a hybrid stochastic methodology based on the colony and kinetic algorithms and Monte Carlo methodology [6].

Figure 3 demonstrates a clustered cut section of YSZ phase of 3D microstructure, using the explained algorithm in section 2. The zero sites belong to other phases.

Clustering of Nickle, YSZ, and void phases are illustrated in Figs. 4, 5, and 6. Considering all clusters of all phases, it is revealed that for each phase there is only one active cluster. Other clusters, in spite of their large size (Fig. 4) or large numbers (of void in Table 1), are not percolated and they have no effect on the performance of SOFC.

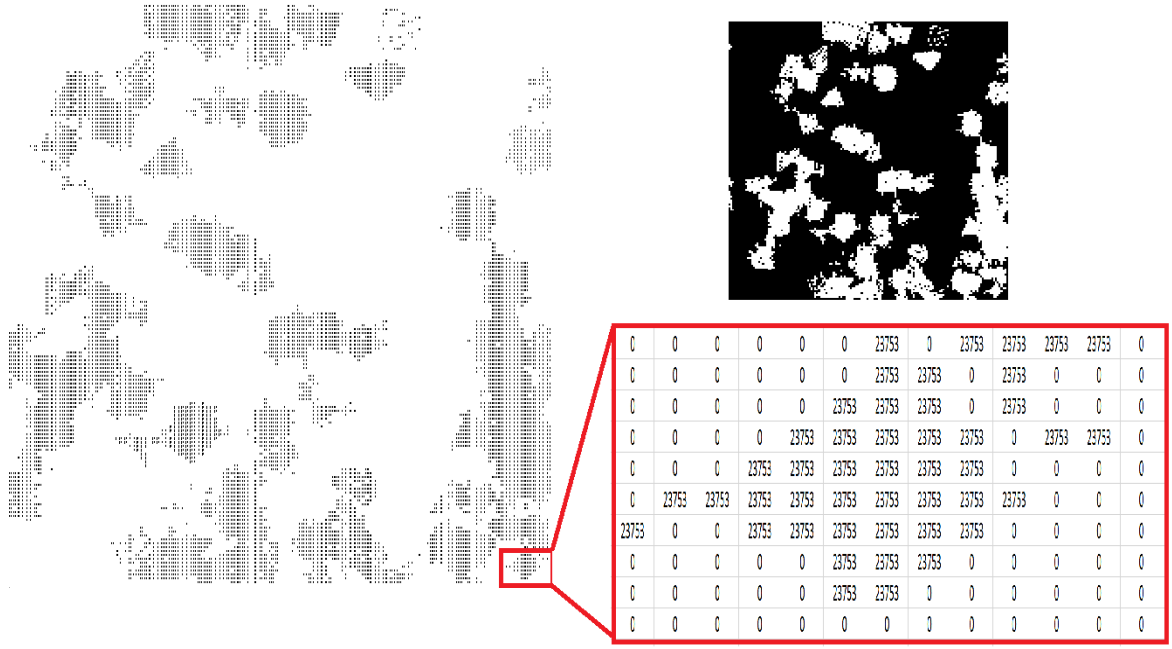

Fig. 3. A 2D cut-section of a 3D 150x150x150 pixel and the respective clustered cells

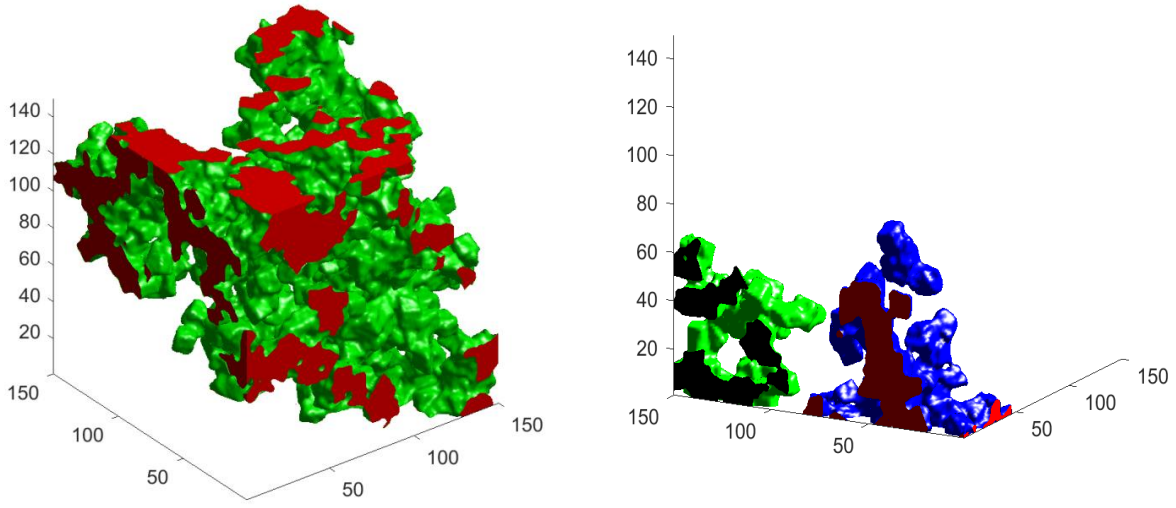

Fig. 4. Cluster of Nickle phase (left) the main percolated cluster (right) the second cluster and third one that are not active

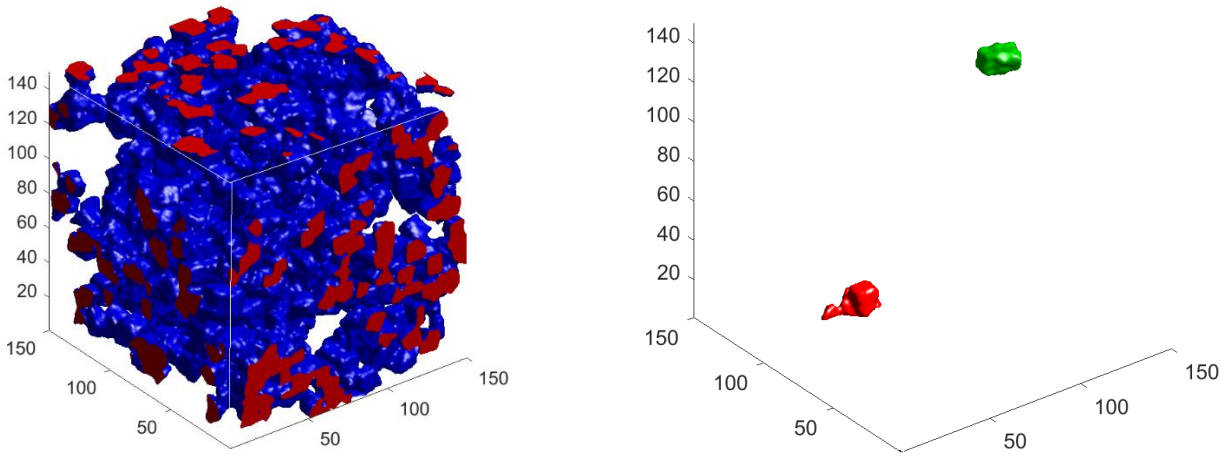

Fig. 5. The cluster of YSZ phase: (left) the main percolated cluster (right) the second cluster and third one. Compared with Nickle phase, these clusters are very small.

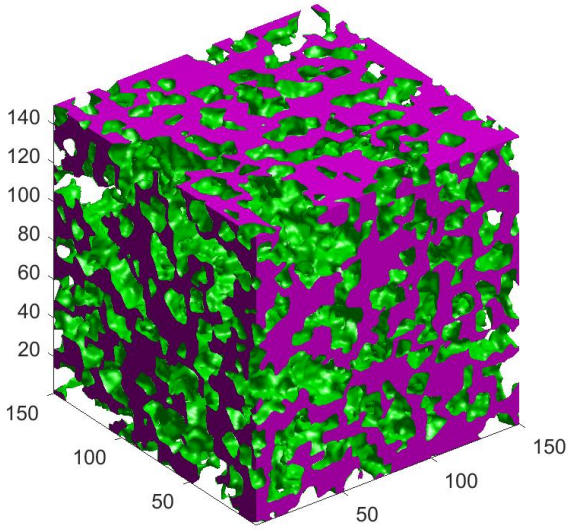

Fig. 6. The main percolated cluster of void phase. Other clusters of this phase are many but their size is very small.

Analysis of the active clusters for all three phases is listed in Table 1.

It could be seen that for the phase with lowest volume fraction, Nickle, there are large inactive clusters. On the other hand, for void, that is the phase with largest volume fraction, there are a large numbers of inactive clusters, but their size is very small (compared to the size of main active cluster).

From the viewpoint of percolation, the best configured phase is YZS. This phase has the largest active percentage and the lowest inactive cluster.

Table 1. Clustering of all three phases (Nickle, YSZ and void). There is only one active cluster for each of phases.

phase	Volume fraction	Number of cells	Number of cluster	Size of active cluster	Size of second cluster	Size of third cluster	Active cluster percent
Nickle	0.26	877,512	442	722,197	43792	35687	82%
YSZ	0.33	1,118,713	309	1,102,001	2231	21015	98.5%
Void	0.41	1,378,775	44,718	1,325,232	147	105	96%

5.2. Counting Active TPBL Segment

Using the proposed method in section 3, the total and active TPB are listed in Table 2. The value for the percentage of active TPB, e.g. 63%, has conformity with the 66.1 % of Ref. [26] (with the same volume fraction for Nickle and YSZ phases). Also, the value of density of TPBL (0.005996) matches that (0.0057-0.0231) reported by Mazrouei et al. [15].

Figure 7 illustrates the active and total TPB segments. The red segments are not attached to the main percolated cluster and are inactive.

5.3. Tortuosity Calculation

Using the Avizo Fire 8.1 software, F and other related parameters were calculated. Applying two different temperatures on two opposite faces and assuming others as adiabatic faces, the effective thermal conductivity is calculated. Tortuosity of all phases is listed in Table 3. The attained amounts are in good agreement with presented values of tortuosity for each phase given by Ref. [27].

When gas diffuses or electrons and ions transport, only the active cells of each phase are being involved. Therefore, if the inactive clusters of each phase were removed, the actual tortuosity of each phase or tortuosity of percolated clusters could be determined as illustrated in Table 3.

Table 2. TPB segment counting of active and total clusters.

Total TPB segment	Active TPB segment	Percent of active TPB	Total cell of microstructure	Density of TPBL (segment/cell)
31986	20237	63%	3,375,000	0.005996

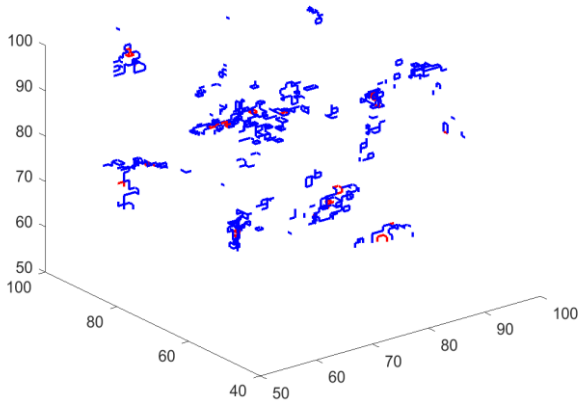

Fig. 7. Active (blue) and total (blue and red) TPB segments

Table 3. Effective thermal conductivity (diffusion) coefficient and tortuosity

phase	Volume fraction	F^{-1}	Tortuosity	Percent of Active	Tortuosity of percolated cluster
Nickle	0.26	0.04453	5.84	21.4	4.81
YSZ	0.33	0.06715	4.91	32.65	4.86
Void	0.41	0.16060	2.55	39.27	2.45

6. Conclusion

In the present study, evaluation of a three-phase SOFC anode based on three-phase boundary and tortuosity was investigated. Clustering of phases and determining the active clusters was carried out using the proposed algorithms. It was revealed that for each phase only one cluster is the main active cluster and other clusters, in spite of their large number or size, are inactive. Also for Nickle, the phase with lowest volume fraction, large inactive clusters were observed. On the other hand, for void, that was the phase with largest volume fraction, large number of inactive clusters existed, but their size was very small. The attained values for TPB and tortuosity are in good agreement with other previous studies.

Using the proposed algorithm, it is possible to identify useless clusters and avoid assigning materials to these unused cells. This can be used in topology optimization for evaluating a proposed topology. Provided 3D print of a microstructure is possible, this algorithm could be used for removing unused clusters and reducing additional cost of material and manufacturing.

7. Acknowledgment

This project was supported by Iranian Gas Transmission Co in financial aspects.

References

[1] Dincer I., Colpan C. O., CHAPTER 1 Introduction to Stationary Fuel Cells, in Solid Oxide Fuel Cells, From Materials to System Modeling, ed: The Royal Society of Chemistry (2013) 1-25, ISBN 978-1-84973-654-1, The Royal Society of Chemistry.

[2] Bove R. and Ubertini S., Modeling Solid Oxide Fuel Cells, Methods, Procedures and Techniques (2014) 3-13, ISBN 9789400796102, Springer Netherlands.

[3] Cronin J. S., Chen-Wiegart Y.-c. K., Wang J., Barnett S. A., Three-Dimensional Reconstruction and Analysis of an Entire Solid Oxide Fuel Cell by Full-Field Transmission X-ray Microscopy, Journal of Power Sources (2013) 233: 174-179.

[4] Lanzini A., Leone P., Asinari P., Microstructural Characterization of Solid Oxide Fuel Cell Electrodes by Image Analysis Technique, Journal of Power Sources (2009) 194: 408-422.

[5] He W., Lv W., Dickerson J. H., Gas Transport in Solid Oxide Fuel Cells (2014) 1-33 ,ISBN 978-3-319-09736-7 , New York: Springer.

[6] Baniassadi M., Garmestani H., Li D. S., Ahzi S., Khaleel M., Sun X., Three-Phase Solid Oxide Fuel Cell Anode Microstructure Realization Using Two-Point Correlation Functions, Acta Materialia (2011) 59: 30-43.

[7] Endo A., Wada S., Wen C. J., Komiyama H., Yamada K., Low Overvoltage Mechanism of High Ionic Conducting Cathode for Solid Oxide Fuel Cell, Journal of The Electrochemical Society (1998) 145: L35-L37.

[8] Song X., Diaz A. R., Benard A., Nicholas J. D., A 2D Model for Shape Optimization of Solid Oxide Fuel Cell Cathodes, Structural and Multidisciplinary Optimization (2013) 47: 453-464.

[9] Baniassadi M., Ahzi S., Garmestani H., Ruch D., Remond Y., New Approximate Solution for N-Point Correlation Functions for Heterogeneous Materials, Journal of the Mechanics and Physics of Solids (2012) 60: 104-119.

[10] Hamedani H. A., Baniassadi M., Khaleel M., Sun X., Ahzi S., Garmestani H., Microstructure, Property and Processing Relation in Gradient Porous Cathode of Solid Oxide Fuel Cells Using Statistical Continuum Mechanics, Journal of Power Sources (2011) 196: 6325-6331.

[11] Ghazavizadeh A., Soltani N., Baniassadi M., Addiego F., Ahzi S., Garmestani H., Composition of Two-Point Correlation Functions of Subcomposites in Heterogeneous Materials, Mechanics of Materials (2012) 51: 88-96.

[12] Amani Hamedani H., Baniassadi M., Sheidaei A., Pourboghrat F., Rémond Y., Khaleel M., et al., Three-Dimensional Reconstruction and Microstructure Modeling of Porosity-Graded Cathode Using Focused Ion Beam and Homogenization Techniques, Fuel Cells (2014) 14: 91-95.

[13] Tabei S. A., Sheidaei A., Baniassadi M., Pourboghrat F., Garmestani H., Microstructure Reconstruction and Homogenization of Porous Ni-YSZ Composites for Temperature Dependent Properties, Journal of Power Sources (2013) 235: 74-80.

[14] Irvine J. T.S., Connor P., Solid Oxide Fuels Cells, Facts and Figures (2013) 1-25 ,ISBN 978-1-4471-4455-7 ,London, Springer-Verlag.

[15] Sebdani M. M., Baniassadi M., Jamali J., Ahadiparast M., Abrinia K., Safdari M., Designing an Optimal 3D Microstructure for Three-Phase Solid Oxide Fuel Cell Anodes with Maximal Active Triple Phase Boundary Length (TPBL), International Journal of Hydrogen Energy (2015) 40: 15585-15596.

[16]Deng X., Petric A., Geometrical Modeling of the Triple-Phase-Boundary in Solid Oxide Fuel Cells, Journal of Power Sources (2005) 140: 297-303.

[17] Janardhanan V. M., Heuveline V., Deutschmann O., Three-Phase Boundary Length in Solid-Oxide Fuel Cells, A Mathematical Model, Journal of Power Sources (2008) 178: 368-372.

[18] Golbert J., Adjiman C. S., Brandon N. P., Microstructural Modeling of Solid Oxide Fuel Cell Anodes, Industrial & Engineering Chemistry Research (2008) 47: 7693-7699.

[19] Suzue Y., Shikazono N., Kasagi N., Micro Modeling of Solid Oxide Fuel Cell Anode Based on Stochastic Reconstruction, Journal of Power Sources (2008) 184: 52-59.

[20] Wilson J. R., Cronin J. S., Duong A. T., Rukes S., Chen H.-Y., Thornton K., et al., Effect of Composition of (La0.8Sr0.2MnO3–Y2O3-stabilized ZrO2) Cathodes, Correlating Three-Dimensional Microstructure and Polarization Resistance, Journal of Power Sources (2010) 195: 1829-1840.

[21] Shikazonoz N., Kanno D., Matsuzaki K., Teshima H., Sumino S., Kasagi N., Numerical Assessment of SOFC Anode Polarization Based on Three-Dimensional Model Microstructure Reconstructed from FIB-SEM Images, Journal of Electrochem. Society (2010) 157: B665-B672.

[22] Iwai H., Shikazono N., Matsui T., Teshima H., Kishimoto M., Kishida R., et al., Quantification of SOFC Anode Microstructure Based on Dual Beam FIB-SEM Technique, Journal of Power Sources (2010) 195: 955-961.

[23] Hoshen J., Kopelman R., Percolation and Cluster Distribution. I. Cluster Multiple Labeling Technique and Critical Concentration Algorithm, Physical Review B (1976) 14: 3438-3445.

[24] Torquato S., Random Heterogeneous Materials, Microstructure and Macroscopic Properties (2002) 355-357 ,ISBN 978-1-4757-6357-7, New York, Springer-Verlag.

[25] Riazat M., Baniasadi M., Mazrouie M., Tafazoli M., Moghimi Zand M., The Effect of Cathode Porosity on Solid Oxide Fuel Cell Performance, Energy Equipment and Systems (2015) 3: 25-32.

[26] Vivet N., Chupin S., Estrade E., Richard A., Bonnamy S., Rochais D., et al., Effect of Ni Content in SOFC Ni-YSZ Cermets, A Three-Dimensional Study by FIB-SEM Tomography, Journal of Power Sources (2011) 196: 9989-9997.

[27] Shikazono N., Kasagi N., CHAPTER 8 Three-Dimensional Numerical Modelling of Ni-YSZ Anode, in Solid Oxide Fuel Cells: From Materials to System Modeling (2013) 200-218, ISBN 978-1-84973-654-1, The Royal Society of Chemistry.